RESEARCH ON SEMICONDUCTORS AT CRYOGENIC TEMPERATURES

G. R. Wagner and M. A. Janocko
Superconductor Materials & Electronics

Final Report for the period
July 1, 1985 to June 18, 1988

Office of Naval Research
Contract No. N00014-85-C-0579

June 26, 1988

Westinghouse R&D Center
1310 Beulah Road
Pittsburgh, Pennsylvania 15235

RESEARCH ON SEMICONDUCTORS AT CRYOGENIC TEMPERATURES

G. R. Wagner and M. A. Janocko
Superconductor Materials & Electronics

Final Report for the period
July 1, 1985 to June 18, 1988

Office of Naval Research
Contract No. N00014-85-C-0579

June 26, 1988

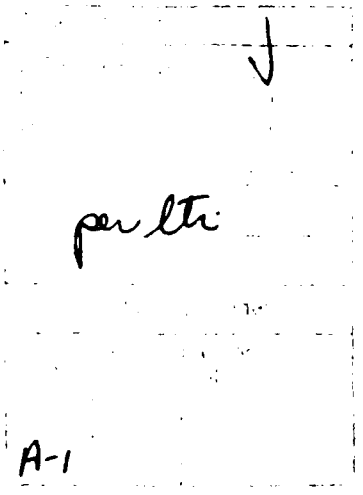

Westinghouse R&D Center
1310 Beulah Road
Pittsburgh, Pennsylvania 15235

CONTENTS

LIST OF FIGURES

LIST OF FIGURES (cont.)

ABSTRACT

The Hall mobility and magnetoresistance of selectively doped heterostructures of Si_xGe_{1-x}/Ge prepared by molecular beam epitaxy (MBE) have been studied in the temperature range $1.5 < T < 300K$. Either Al or B was used to dope the alloy p-type. Evidence was found in the B-doped samples with $x = 0.5$ that a 2DHG is formed in the Ge at the heterointerface. The mobility at $T = 4.2K$ in a sample with an undoped alloy spacer layer of 4 nm was $\mu_H = 3.2 \times 10^3$ cm^2/V-sec and in other samples was found to decrease with spacer layer thickness. Shubnikov-de Haas oscillations were observed at $T = 1.5K$ with the magnetic field normal to the interface, but not with the field parallel to it. The oscillation period yields a surface charge density of $2 \times 10^{12}/cm^{-2}$ in reasonable agreement with the value of $3 \times 10^{12}/cm^{-2}$ obtained by Hall measurements.

1. INTRODUCTION

The need for high-speed, low-power, low-noise electronic devices for use in signal processing and computer applications has generated interest in the behavior of semiconducting devices at cryogenic temperatures because an increase in speed and a reduction in noise are obtained by cooling them. Carrier freeze-out prevents bipolar transistors from working at cryogenic temperatures, but field effect devices, when properly doped, do not suffer carrier freeze-out and show expected performance improvements at low temperatures.[1] Modulation-doped heterostructures show an even greater improvement. The high electron mobility transistor (HEMT), also known as the modulation-doped FET (MODFET), made from a GaAs/AlGaAs heterostructure has a higher transconductance, higher carrier mobility, and lower parasitic capacitance than the Si MOSFET at room temperature and demonstrates a remarkable improvement in switching speed at cryogenic temperatures. This increase in speed results from the spatial separation of the carriers in the conducting channel and the ionized donors. The separation reduces the Coulomb scattering and increases the carrier mobility leading to higher carrier velocities.

Heterostructure devices utilizing GaAs/AlGaAs as well as other III-V compounds, their ternarys, and quartenarys have been studied for several years. Modulation-doped structures and quantum-well devices are being used to develop many novel electronic and opto-electronic devices. Most all of them show enhanced performance from, or actually require, low-temperature operation. A dramatic example is the recently developed GaAs/AlGaAs ballistic transistor,[2] which surpasses even the HEMT in speed.

However, the GaAs materials base suffers from some disadvantages, and a MCDFET based on the more mature Si-based technology would allow the incorporaion of higher speed devices onto Si chips with the inherent advantages of being able to meld them with existing, well-understood Si devices.

The purpose of this program was to investigate the low-temperature properties of heterostructures made in the Si-Ge materials system to determine whether two-dimensional hole (2DHG) or electron (2DEG) gasses could be formed in strained layer epitaxial structures, and subsequent device improvements made by utilizing their high mobilities at low temperatures.

We began by suggesting that a MODFET-type device could be made by growing a doped epitaxial film of Si_xGe_{1-x} on Ge. In analogy with the GaAs/AlGaAs structure, a two-dimensional gas would be formed in the smaller gap material, Ge. Both electrons and holes in pure Ge have significantly higher mobilities[3] than in Si. In Ge they approach 1×10^6 cm^2/V-sec at T < 20K and thus rival those of electrons in the GaAs HEMT. Since the start of this program, a great deal of interest has been shown by other laboratories in this field. MODFET structures of Ge_xSi_{1-x}/Si have been demonstrated with both p- and n-channel conduction.[4,5] Devices utilizing these structures show improved performance over MOSFETs. Heterostructures which form two-dimensional gasses in Ge should show even greater improvement, and thus we have continued our study of Si_xGe_{1-x}/Ge.

We have concentrated our work on the growth and characterization of p-type alloys on Ge substrates. Si_xGe_{1-x} alloys were grown by MBE on single-crystal wafers of Ge, and the alloys were doped with either Al or B. We have seen evidence for a 2DHG in the B-doped structures with x = 0.5 through the observation of Shubnikov-de Haas oscillations at T = 1.5K. The hole mobility varies with the undoped spacer layer thickness, and the maximum value observed was $\mu_H = 3.2 \times 10^3$ cm^2/V-sec at T = 4.2K for a spacer thickness of 4 nm. The oscillations are observed with the magnetic field perpendicular to the interface but disappear with the field parallel, which is evidence that the degenerate gas is two-dimensional.

We have not attempted to grow n-type layers because of an inability to incorporate n-type dopants in our MBE system.

2. EXPERIMENTAL

2.1 MBE APPARATUS

The Si_xGe_{1-x}/Ge heterostructures were grown epitaxially on Ge wafers in a commercial high-vacuum system which has been fully described elsewhere.[6] A schematic view of the system describing each chamber is shown in Figure 1. The deposition and analysis chambers have a base pressure in the low-10^{-11} Torr range.

Molybdenum sample blocks which may be rotated and heated as high as 1200°C during deposition accommodate two-inch diameter wafers. The Ge was evaporated from an effusion cell with the rate controlled by controlling the cell temperature. Two Si sources in two separate e-beam evaporators were used. One contained Si doped with approximately 10^{20} cm^{-3} boron for growing doped alloys, and the other contained pure Si. A third e-beam evaporator was used to provide the Al for doping of the alloys when Al was the dopant of choice. The evaporation rates from the e-beam-heated sources were controlled automatically through the use of quartz crystal monitors. Initially, growth rates of both Si and Ge as a function of substrate temperature and source conditions were determined by measuring layer thickness with a profilometer after growth on several Ge wafers. These results were used to determine conditions for growing various alloy compositions, and the final alloy compositions were checked by in-situ XPS and ex-situ electron microprobe.

Reflection high-energy electron diffraction (RHEED) in the deposition chamber and low-energy electron diffraction (LEED) in the analysis chamber were used to determine the surface quality of the substrates and the crystalline quality of the grown films.

2.2 WAFER PREPARATION AND CHARACTERIZATION

Two-inch diameter single-crystal wafers (0.023 inch thick) of high-purity Ge with a (100) orientation were obtained from Eagle-Picher

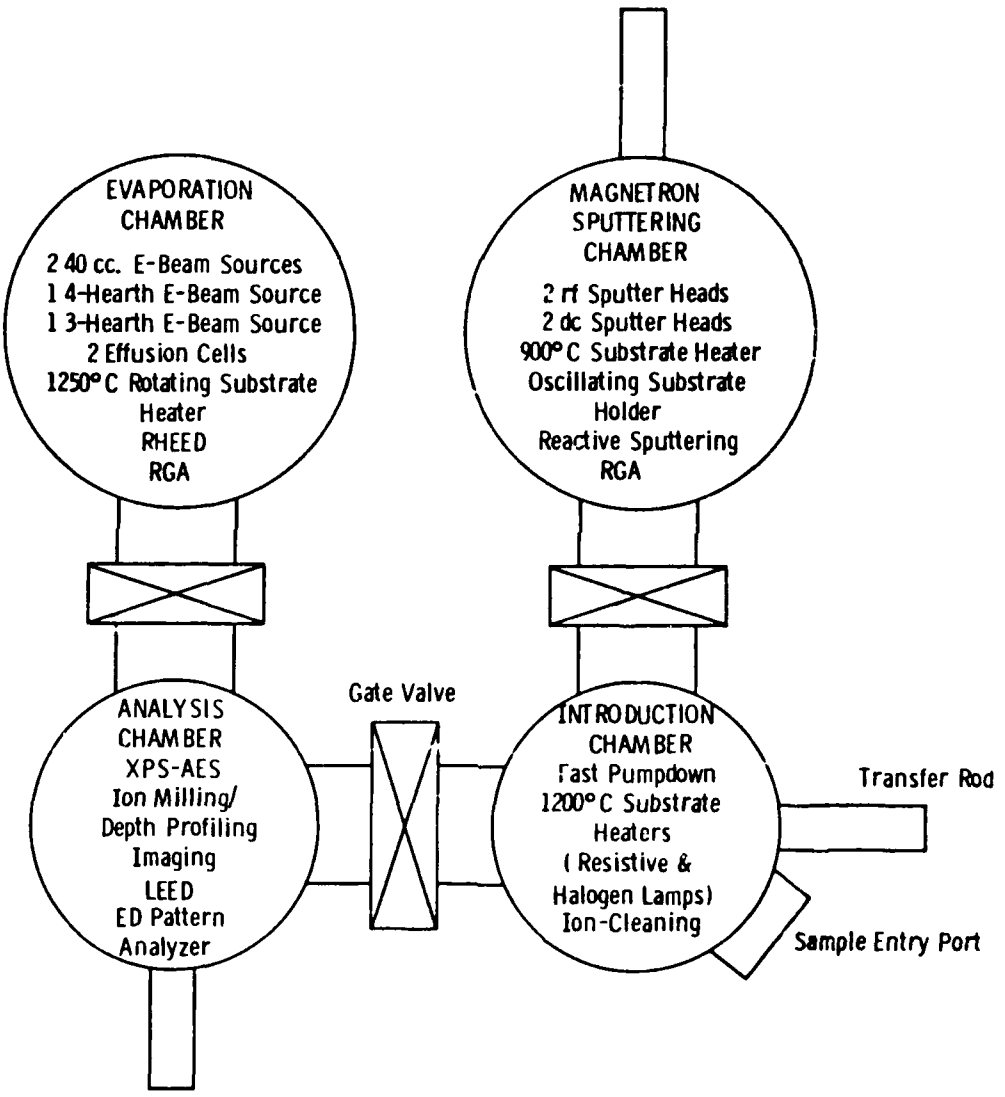

Figure 1. Schematic of the UHV MBE superlattice deposition and facility (SDAF) and magnetron sputtering chamber.

Corp. and polished on one side by Semiconductor Processing, Inc. The room-temperature resistivity was specified to be greater than 40 ohm-cm, and this was verified by our measurements. The wafers were p-type due to a residual boron impurity concentration of $\simeq 10^{13}$ cm^{-3}.

The wafers were cleaned prior to placement in the MBE system by a procedure described by Aspnes and Studna.[7] The procedure involves degreasing in clean methanol, followed by a bromine-methanol pad polish, a bromine-methanol strip, a buffered HF rinse, and a final water rinse. The wafers were blown dry and mounted quickly on the moly block and placed in the introduction chamber of the MBE system.

The wafers were degassed in the introduction chamber at about 300°C. Contaminants were removed from the wafer surface, and the surface was reconstructed by heating in the deposition chamber to a temperature between 600 and 800°C. Good surface reconstruction was obtained as shown by RHEED and LEED patterns. In-situ XPS was used to search for and determine the presence of contaminants such as oxygen, carbon, and fluorine before and after annealing. All were below detectable limits after the high-temperature anneal.

2.3 ELECTRICAL MEASURING APPARATUS

Hall effect, resistivity, and magnetoresistance measurements were performed using a probe which allows temperature control of the sample between room temperature and 4.2K. A second probe, which allows the sample to be immersed in pumped liquid helium, was used to observe the Shubnikov-de Haas oscillations at T = 1.5K. In the variable temperature probe, the sample was mounted on a copper block inside of a can which were immersed in liquid helium or nitrogen. A heater and two thermometers were thermally anchored to the block. A carbon-glass resistance thermometer was used for $T < 15K$ and a platinum resistance thermometer for $T > 15K$. The carbon glass was purchased with calibration from Lakeshore Cryotronics, Inc., and the Pt resistor was obtained from Lakeshore but calibrated in-house. The temperature was measured with a SHE, Inc. Model PCB conductance bridge.

With the can evacuated the sample temperature was controlled by varying the input power to the heater. The sample was electrically isolated from the block by a 0.015-inch thick piece of single-crystal sapphire. For temperatures between 4.2 and 10K, a small amount of helium exchange gas was admitted to the can to ensure thermal equilibrium between the sample and the thermometers.

The Hall and resistivity measurements were made by the standard four-point Van der Pauw method. The samples were either square (0.25 inch) or cloverleaf-shaped cut from the square with a cavitron.

Most of the Hall measurements were made in a magnetic field of 0.2 T provided by a superconducting NbTi magnet which has a maximum field of 3 T. The probe could also be used in a second NbTi magnet providing up to 6 T. Some measurements were made in this magnet to determine the field dependence of the Hall effect. Magnetoresistance measurements were made to study the Shubnikov-de Haas oscillations in a Nb_3Sn magnet with a two-inch bore capable of producing 15 T. A stainless steel insert dewar allowed the sample to be immersed in pumped helium without pumping on the large reservoir of helium cooling the magnet. A minimum temperature of 1.5K was obtained with the available pumps. The temperature was determined from the helium vapor pressure.

2.4 SAMPLE PREPARATION

Samples were cut from the two-inch wafers after epitaxy by two techniques; either diamond wheel sawing or cavitroning. Photoresist was spun on the wafer for surface protection during sawing. A layer of beeswax was applied over the photoresist for adequate protection during cavitroning. Hall and resistivity samples were sawed squares or cavitroned cloverleafs. The Shubnikov-de Haas samples were saw-cut bars 0.50 inch long by 0.05 inch wide.

Ohmic contacts were made by alloying indium on the surface at 300°C in a reducing atmosphere. Contacts were made on the corners of the squares, to the leafs of the cloverleafs, and to the ends and sides of the bars.

3. RESULTS AND DISCUSSION

3.1 EPITAXIAL FILM GROWTH

Following cleaning by the Aspnes and Studna[7] technique, degassing in the introduction chamber, and surface reconstruction by high-temperature anneal, the wafer surface was investigated by RHEED, LEED, and in-situ XPS. Many runs were made but here only typical results are shown.

Figure 2 is a LEED pattern of a (100) surface of a Ge wafer following a 600°C anneal. The pattern shows sharp spots and a 2 x 1 surface reconstruction. Figure 3 is a RHEED pattern for the same wafer after annealing. This pattern is characteristic of a smooth surface. In particular, the observed Kikuchi lines indicate a surface of excellent quality and smoothness.

In-situ XPS data of a wafer before and after reconstruction at 750°C are shown in Figure 4. The oxygen peak is clearly visible before annealing and absent after. Similar results were obtained for carbon and fluorine.

After reconstruction of the wafer surface, a buffer layer of pure Ge was deposited on the wafer to further improve the quality of the surface for epitaxial growth of the alloy. The buffer layer thickness was in the range of 100 to 500 nm. Figures 5 and 6 show RHEED and LEED patterns of a 100 nm thick buffer, which indicate good crystalline quality and that the buffer grew epitaxially.

The alloy layers were deposited by co-evaporation of Si and Ge. Setback layers of undoped Si_xGe_{1-x} were grown by using the pure Si e-beam source. Figures 7 and 8 show RHEED and LEED patterns of 100 nm of $Si_{0.15}Ge_{0.85}$ on the 100 nm of pure Ge buffer shown in Figure 5. The alloy layer was deposited at a substrate temperature of 550°C. The doped alloy layers were grown using the B-doped Si source or the undoped

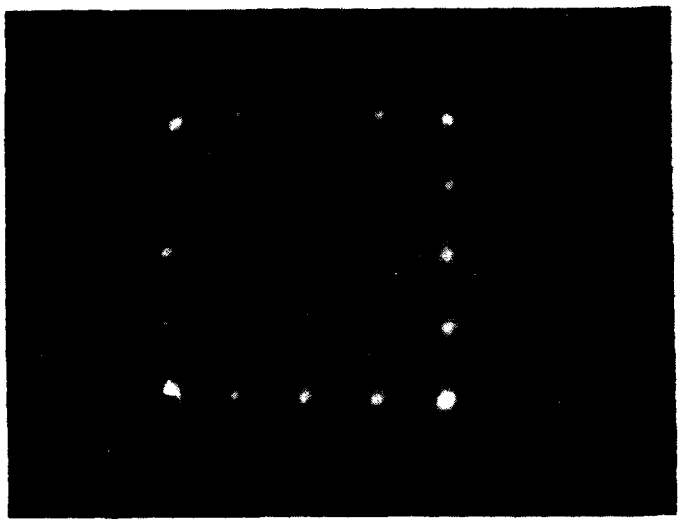

Figure 2. LEED pattern at 43 volts of (100) surface of Ge wafer after 600°C anneal.

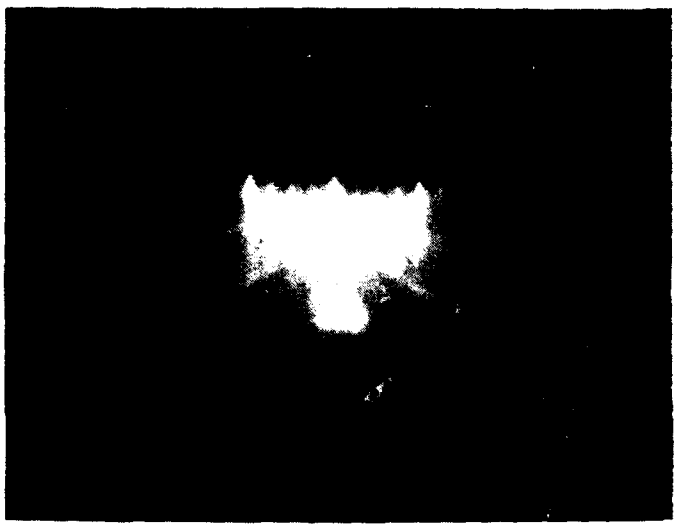

Figure 3. RHEED pattern of (100) surface of Ge wafer after 600°C anneal.

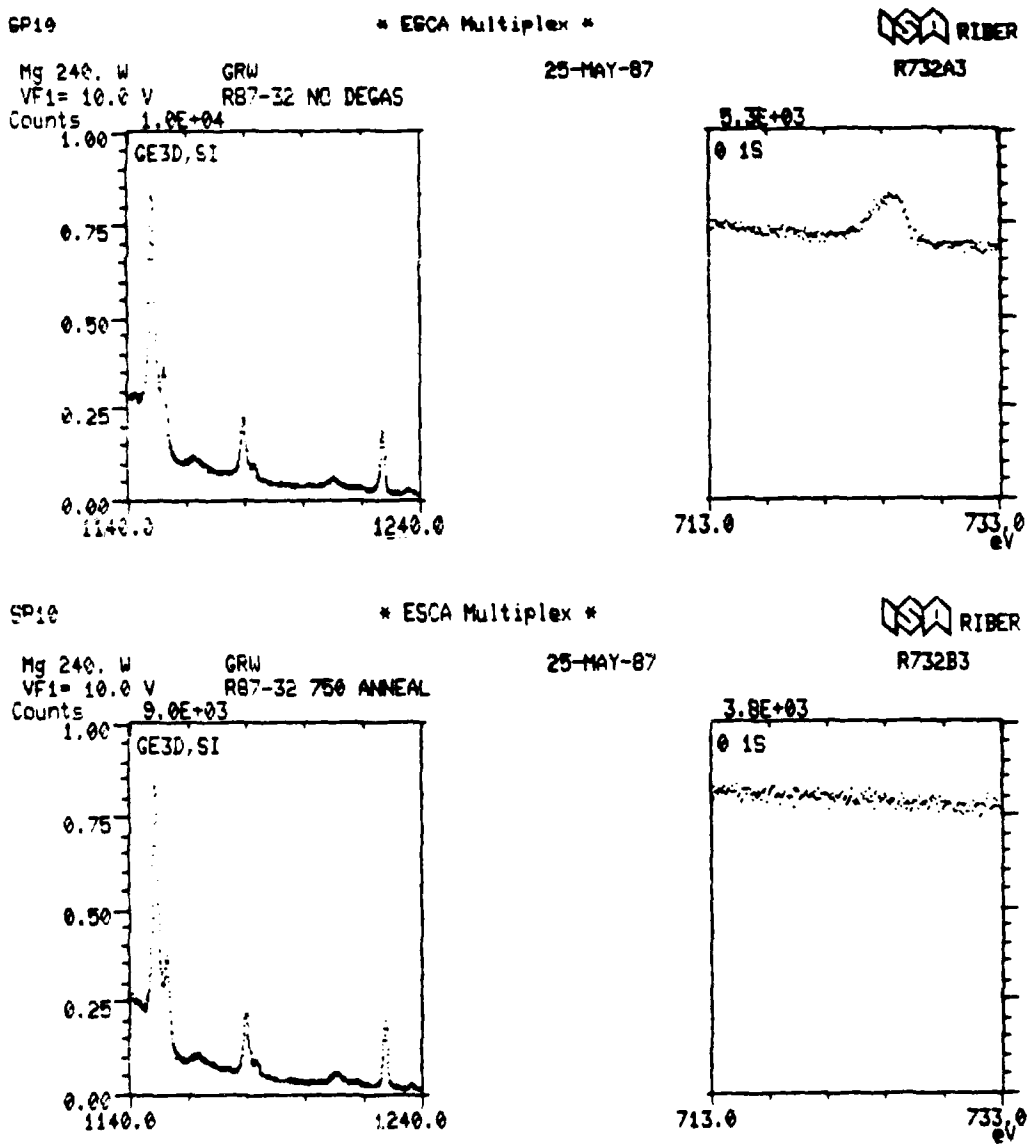

Figure 4. In-situ XPS spectra of (100) Ge wafer before and after 750°C anneal showing removal of oxygen from surface.

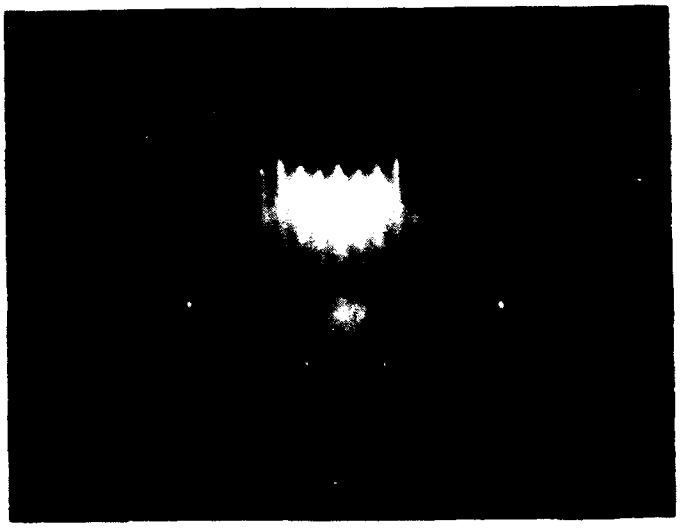

Figure 5. RHEED pattern of surface following deposition of 100 nm of pure Ge on (100) wafer.

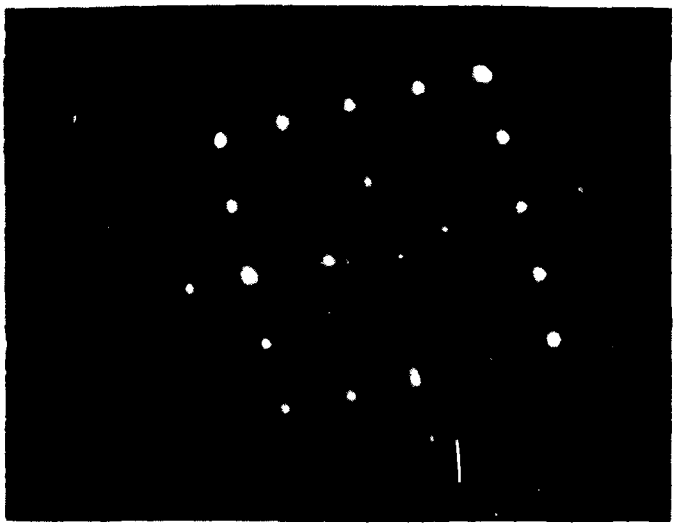

Figure 6. LEED pattern at 44 volts of same surface as in Figure 5.

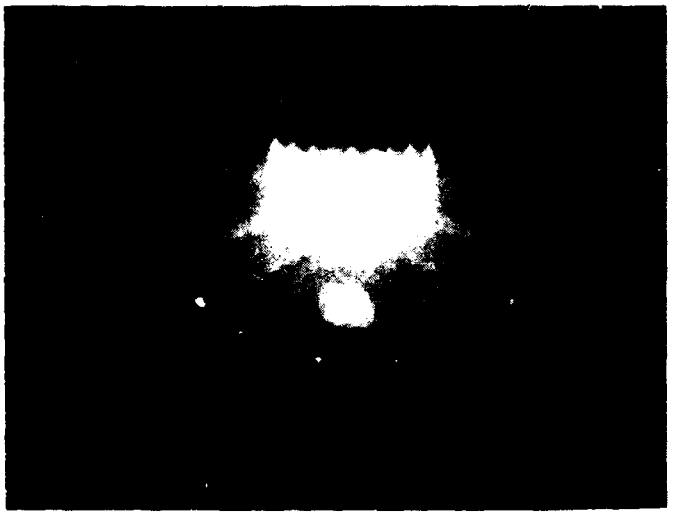

Figure 7. RHEED pattern of surface following deposition of 100 nm of undoped $Si_{0.15}Ge_{0.85}$ on surface of Figure 5.

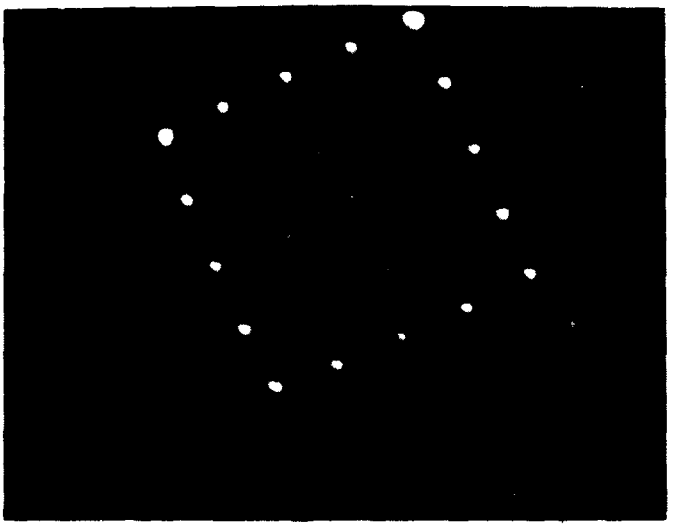

Figure 8. LEED pattern at 44 volts of same surface of Figure 7.

source, with Al being introduced from a separate e-beam source during deposition. In both cases the RHEED and LEED patterns were used as an indication of film quality. Successful films had patterns similar to those in Figures 7 and 8.

3.2 DOPANT INCORPORATION

The starting material for the B-doped alloys was a Si boule doped to a concentration of about 10^{20} cm^{-3}. It had a room-temperature resistivity of 7.5×10^{-4} ohm-cm. It has been shown[8] that high doping levels of B may be obtained in MBE layers by using a Si source which is supersaturated with B. In that method the B-doped Si was sublimed from a boron nitride crucible at various temperatures between 1000 and 1400°C, producing doping levels in the film up to 1.5×10^{20} cm^{-3}. No evidence was found for significant segregation of the B and Si at the surface of the subliming source. However, in our case we expected that melting the doped source might produce different results. Since we wanted to obtain doping levels of 10^{17} to 10^{18} cm^{-3}, a highly doped source was used to compensate for any segregation in the melt or the disparity in sticking coefficients.

The B concentration in the resulting films was determined by SIMS (performed by Charles Evans Associates, Inc., San Mateo, CA) and by spreading resistance measurements. For the latter method, films were deposited on Si substrates which allowed standard techniques to be used in analyzing the data. The concentration in a film grown on Si at a substrate temperature of 800°C was obtained by both methods. The data are shown in Figures 9 and 10. Approximately 250 nm of film were grown at a rate of 12 nm/min followed by 250 nm at a rate of 2.4 nm/min. The spreading resistance data indicate that there was some growth rate dependence to the achieved doping level with the faster rate producing about twice the concentration of B. However, the SIMS data show no such dependence. Furthermore, there is an order of magnitude discrepancy in the concentration obtained by the two methods, which is unexplained. Charles Evans Associates specify that their results are accurate to within a factor of two, and we expect that our spreading resistance

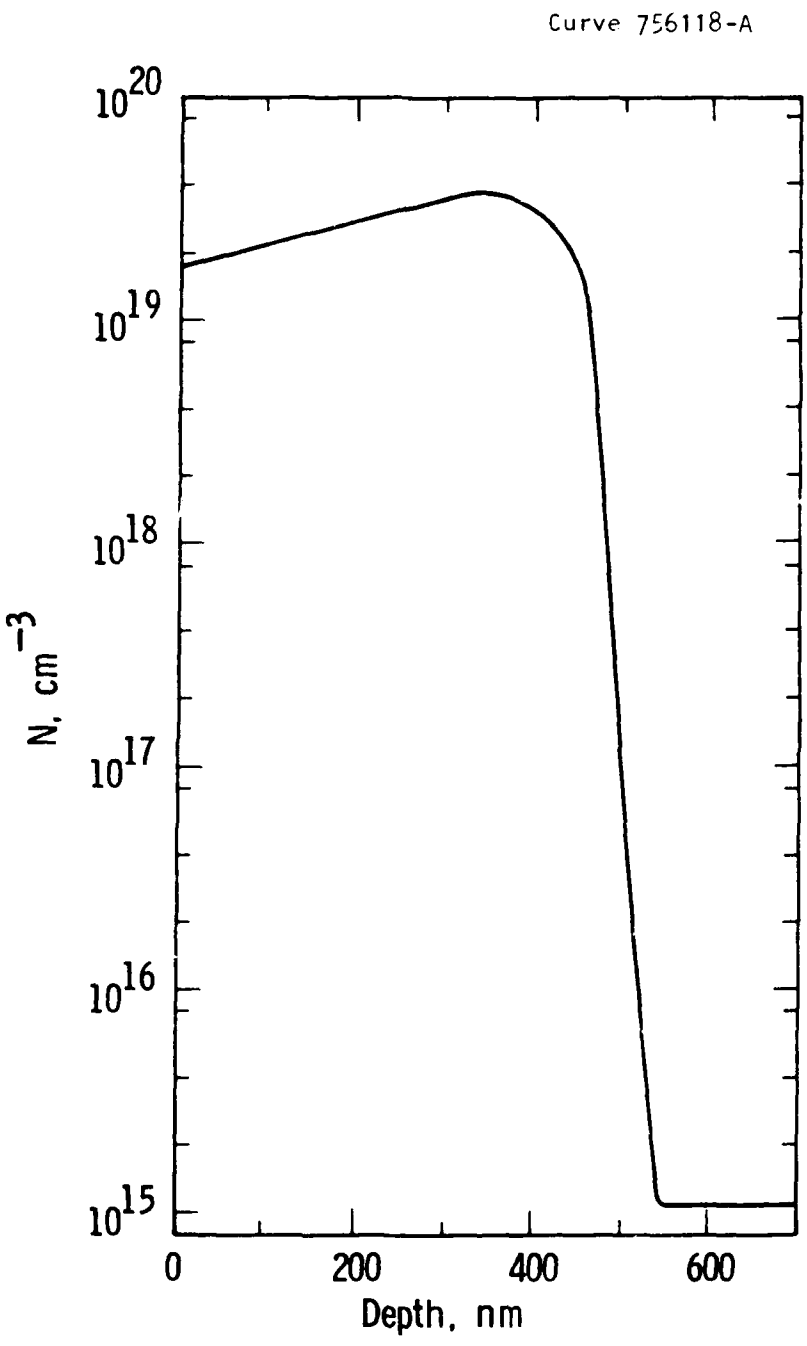

Figure 9. Carrier concentration depth profile obtained from spreading resistance. Sample had 500 nm of doped Si on (100) intrinsic Si wafer.

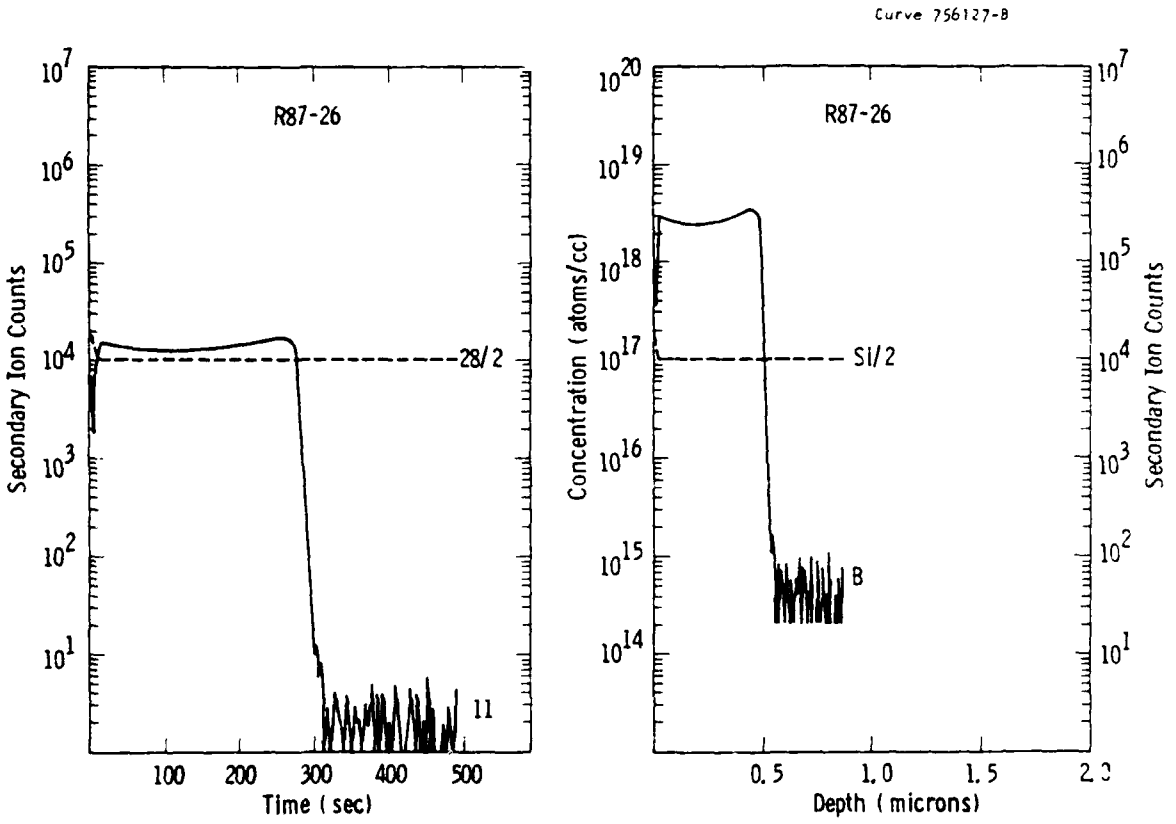

Figure 10. Boron concentration depth profile by SIMS analysis for same sample as Figure 9.

results are good to within a factor of three. The discrepancy is outside the experimental error. A smaller spreading resistance concentration would be obtained if not all the B were electrically active, but it is larger than that indicated by SIMS. In any event, the data indicate that high levels of B doping may be achieved by this method in Si MBE. The data in Figure 9 show a sharp doping profile and indicate that our growth rates are well defined.

Spreading resistance could not be used to obtain the B concentration in the doped alloys. However, a SIMS analysis was done for a film structure consisting of a 100 nm buffer of Ge on a Ge wafer, followed by 10 nm of doped $Si_{0.15}Ge_{0.85}$, and capped by 200 nm of pure Ge. The raw SIMS data are shown in Figure 11. The 10 nm thick doped layer shows clearly about 200 nm below the surface with a spike in the Si and B concentrations. However, the second peak in the B profile is unexpected and unexplained. It is unlikely that the B would diffuse into the buffer layer but not into the cap layer. It is possible that the buffer layer was contaminated in some way during growth, but highly unlikely. It is more probable that the second peak is an artifact of the SIMS measurement because the doped layer is thinner than the expected resolution. The results indicate, however, that we are able to obtain high dopant concentrations in these thin alloy layers by the method of using a doped source.

Before the doped Si source was available in the deposition chamber, attempts were made to use the available Al as a dopant. The Al e-beam was adjusted to yield the lowest evaporation possible which could still be controlled by the crystal monitor. This produced much too high a concentration of Al if done continuously during the alloy deposition. To reduce the concentration, the Al was deposited as a dopant spike in various positions in the layer. The Al shutter was opened for a length of time which deposited less than a monolayer. No analysis was done to determine the Al concentration. RHEED and LEED patterns were observed after the dopant spikes were incorporated which indicated that the film quality was not compromised by the presence of the Al.

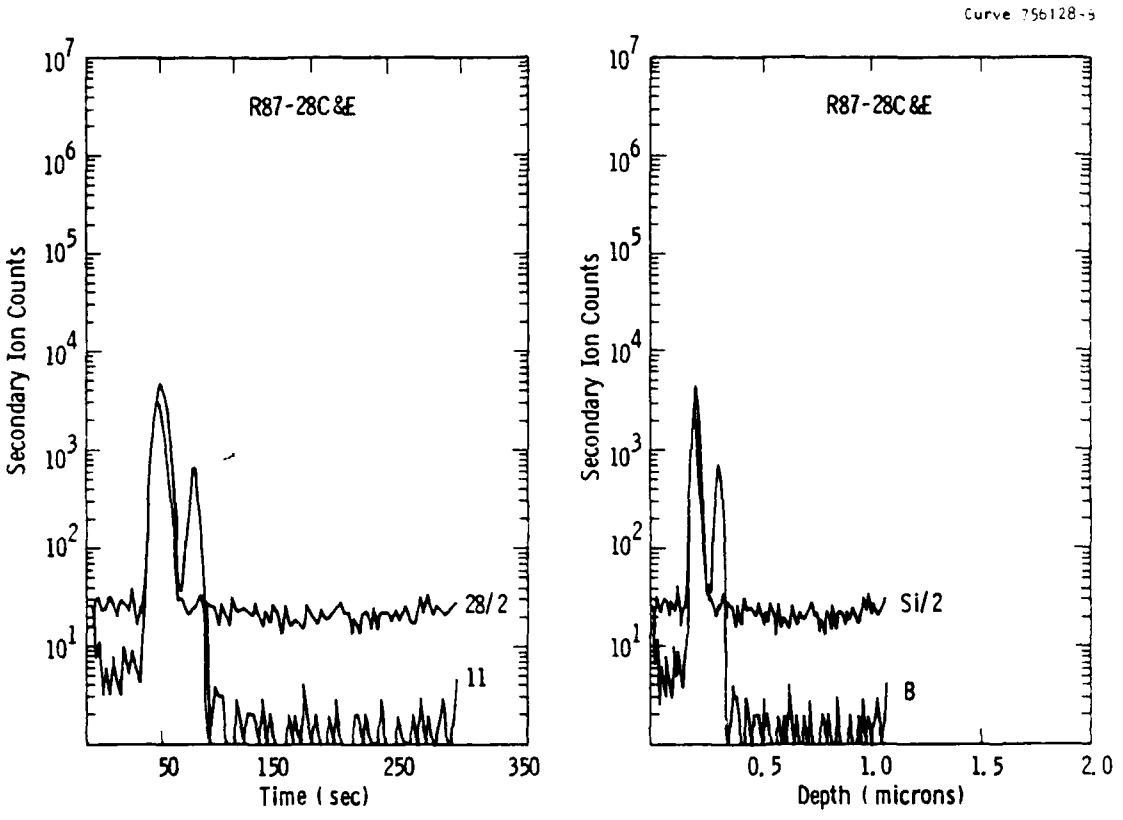

Figure 11. Depth profile of boron concentration by SIMS for sample consisting of 200 nm Ge cap layer on 10 nm of doped $Si_{0.15}Ge_{0.85}$ on 100 nm of Ge buffer on (100) Ge wafer.

3.3 ELECTRICAL TRANSPORT MEASUREMENTS

The following subsections discuss the results of resistivity, Hall effect, and magnetoresistivity measurements on the substrates and heterostructures doped with Al and B. Many samples of various layered configurations were investigated, but only representative samples will be discussed.

3.3.1 Substrate Properties

Samples were cut from two of the supply of Ge wafers used in these experiments and the transport properties measured. The results were the same for both. Figure 12 shows the resistivity and Hall coefficient for one of the samples as a function of reciprocal temperature. The sign of R_H is positive throughout the entire temperature range, and the exponential slope at low temperatures is indicative of the activation energy of the residual boron impurities.

The Hall mobility calculated from R_H and ρ, the resistivity, is shown in Figure 13. The peak mobility occurs near T = 10K at a value of $\mu_H = 4 \times 10^5$ cm^2/V-sec. For T < 10K the mobility decreases rapidly and becomes immeasurably small as the carriers freeze out, and conduction is by hopping. The mobility reaches a value of 10^5 cm^2/V-sec near T = 60K, which is much larger than in heavily doped Si MOSFETs. Such a value, if achieved in a 2DHG, would lead to a significant improvement in switching speed.

3.3.2 Al-doped Structures

When beginning our studies of the Al-doped structures, we chose to use an alloy of 15% Si for two reasons. For Si concentrations of 15% or less, the alloy remains Ge-like with conduction band minima along the [111] directions. This means that the strain-induced splitting of the conduction bands would be absent since all the [111] directions are equivalent for a [100] growth direction. In addition, the results of Bean et al.[9] showed that for alloys containing less than 15% Si, thicknesses of 800 nm and greater could be grown with commensurate epitaxy.

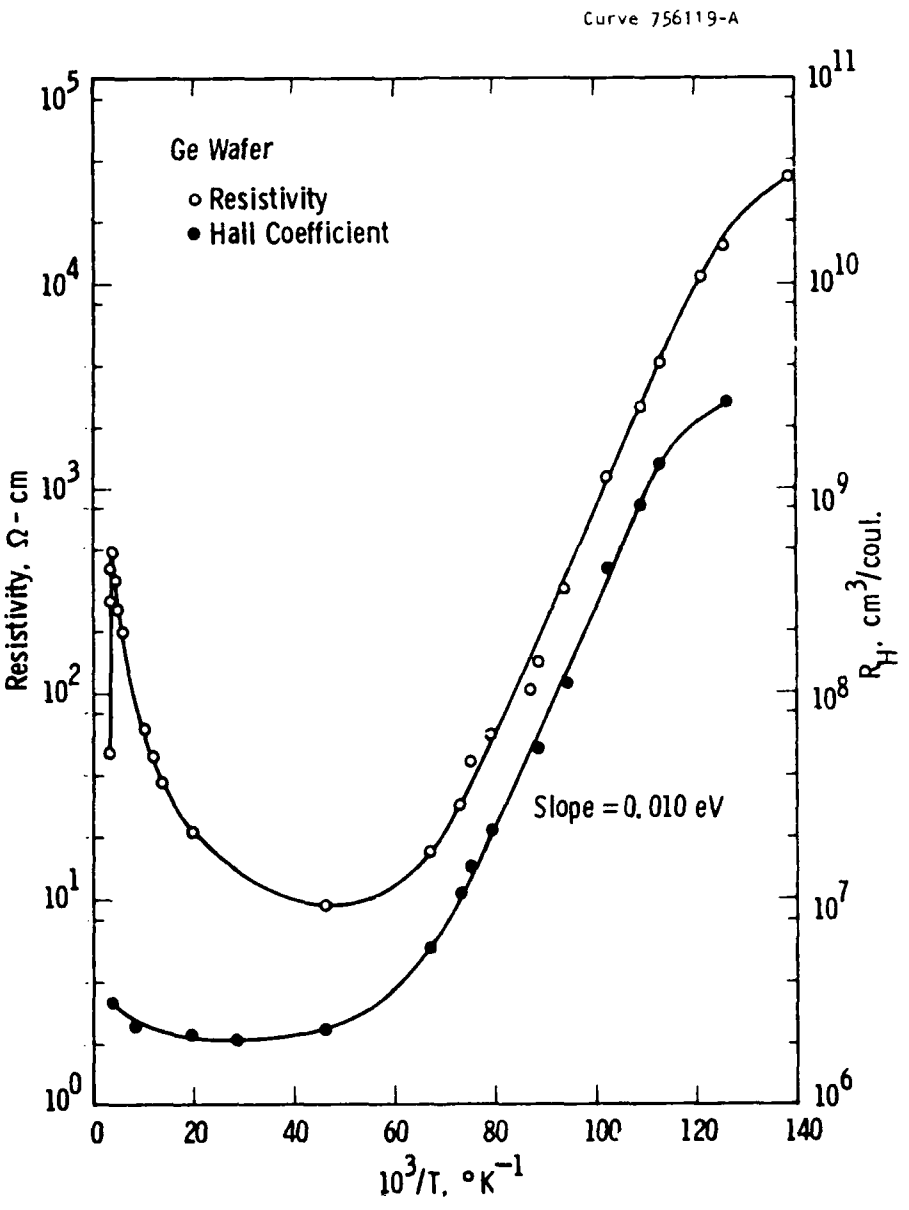

Figure 12. Resistivity and Hall coefficient versus reciprocal temperature for a Ge (100) wafer sample. The magnetic field was normal to the (100) surface for the Hall measurements.

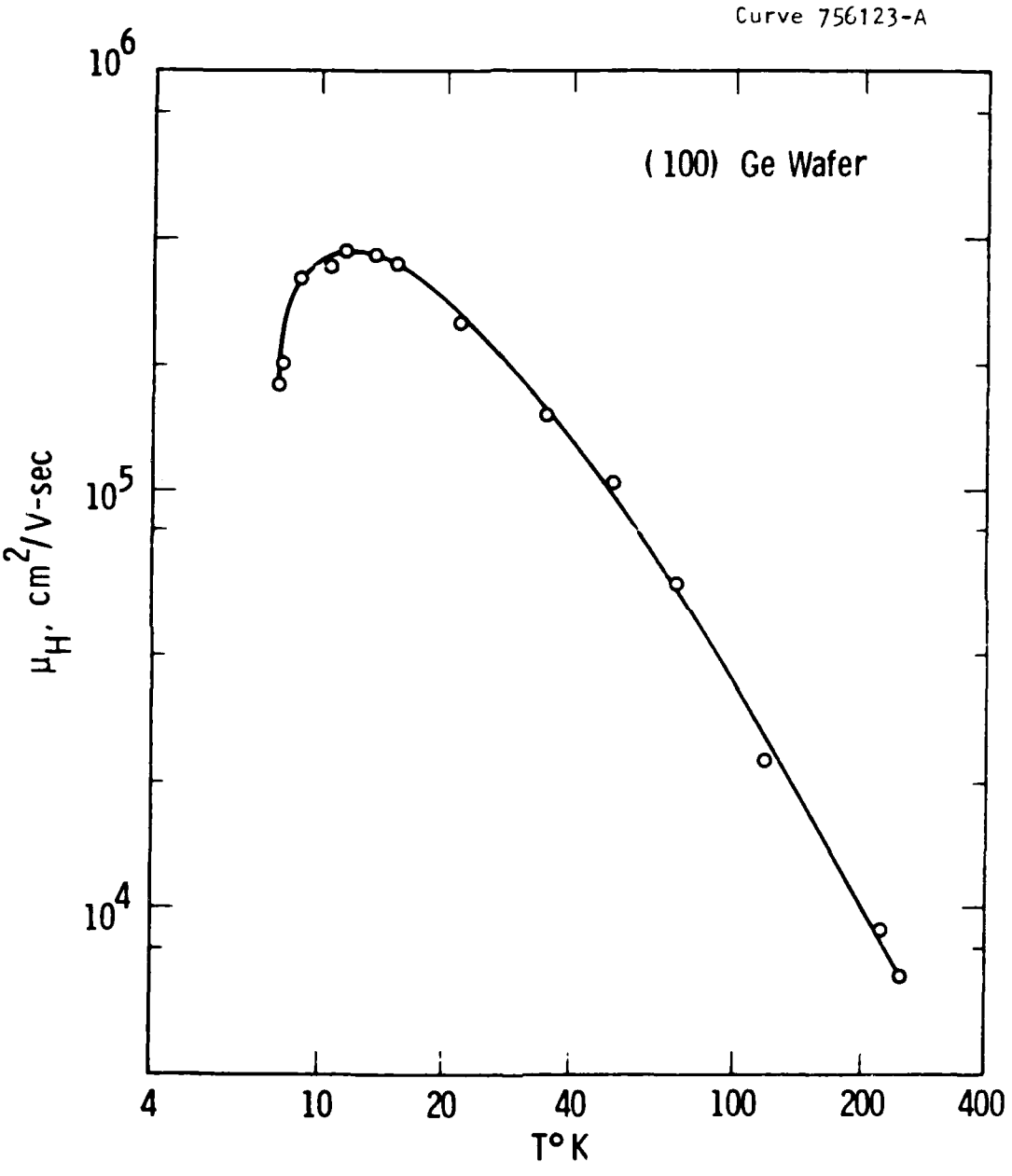

Figure 13. Hall mobility of Ge calculated from data of Figure 16.

Several attempts were made to grow films of $Si_{0.15}Ge_{0.85}$ doped with Al on Ge to obtain a 2DHG in the Ge, although none were successful. Figure 14 shows the Hall mobility calculated from raw data of Hall voltage and resistance for one of the samples, which consisted of 25 nm of alloy doped with four spikes of Al at 5 nm separation during the deposition. The dopant spikes were put in at the lowest concentration possible using our e-beam source. Also shown for comparison is the mobility of the wafer. The room-temperature mobility of the alloy structure is much lower than that of the wafer, but rises to a value of 7.5×10^4 cm^2/V-sec at T = 20K and remains relatively constant as the temperature is lowered to T = 8K. Below T = 7.5K the mobility decreases rapidly.

Figure 15 plots the resistance of the substrate sample and that of the doped alloy sample in ohms per square. Over the entire temperature range the alloy sample has a lower resistance than the wafer and, for T < 15K, its resistance is very much lower. This behavior is typical of the Al-doped samples using a 15% Si alloy of varying thickness, between 25 and 100 nm, and one or more dopant spikes. There is no evidence of a 2DHG, and the data simply imply that we are observing conduction in the bulk alloy in parallel with the substrate. For T < 12K the conduction is dominated by the alloy layer as the carriers freeze out in the substrate.

The mobility calculated for T > 8K is not a true indication of the mobility in either the substrate or the alloy. The measured Hall voltage results from a very large voltage generated in the substrate due to the small concentration of carriers, and a much smaller voltage in the alloy. The different voltage generates a circulating current which causes the measured voltage to be intermediate to the two. However, for T < 7.5K, the carriers in the substrate are sufficiently reduced in number and the resistance so large that the resulting Hall voltage is due to the alloy alone. For the data of Figure 15 we find at T = 4.2K that μ_H = 65 cm^2/V-sec, and the sheet carrier concentration is

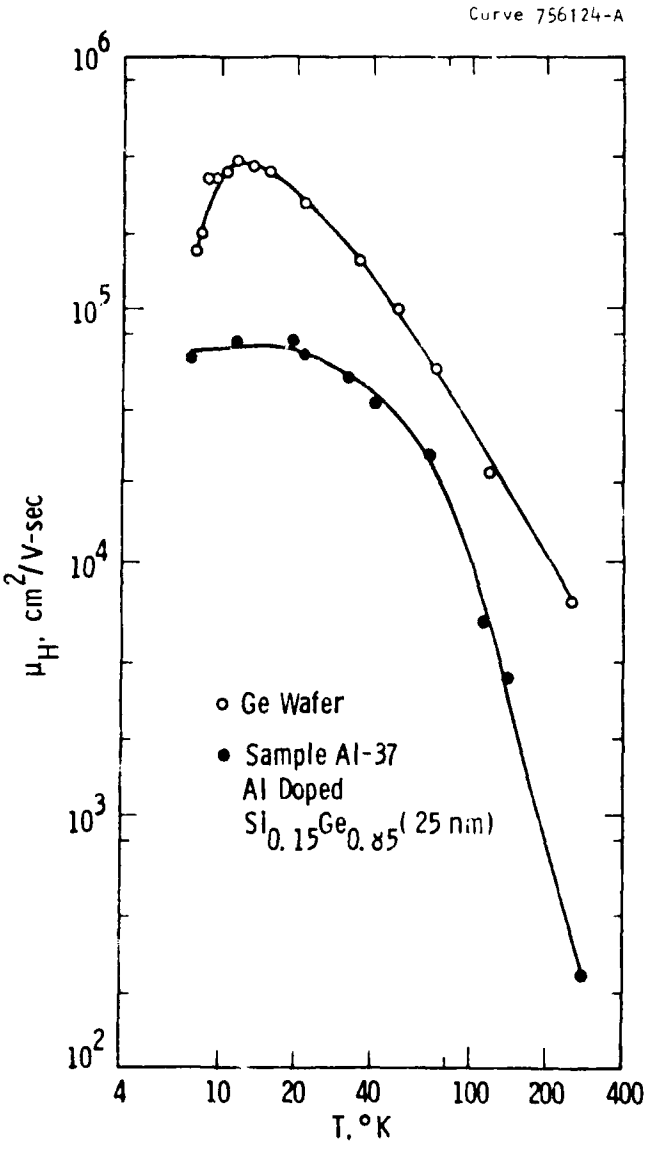

Figure 14. Hall mobility versus temperature for a sample having 25 nm of Al-doped $Si_{0.15}Ge_{0.85}$ on Ge. Magnetic field was normal to (100) surface (plane of epitaxial layer).

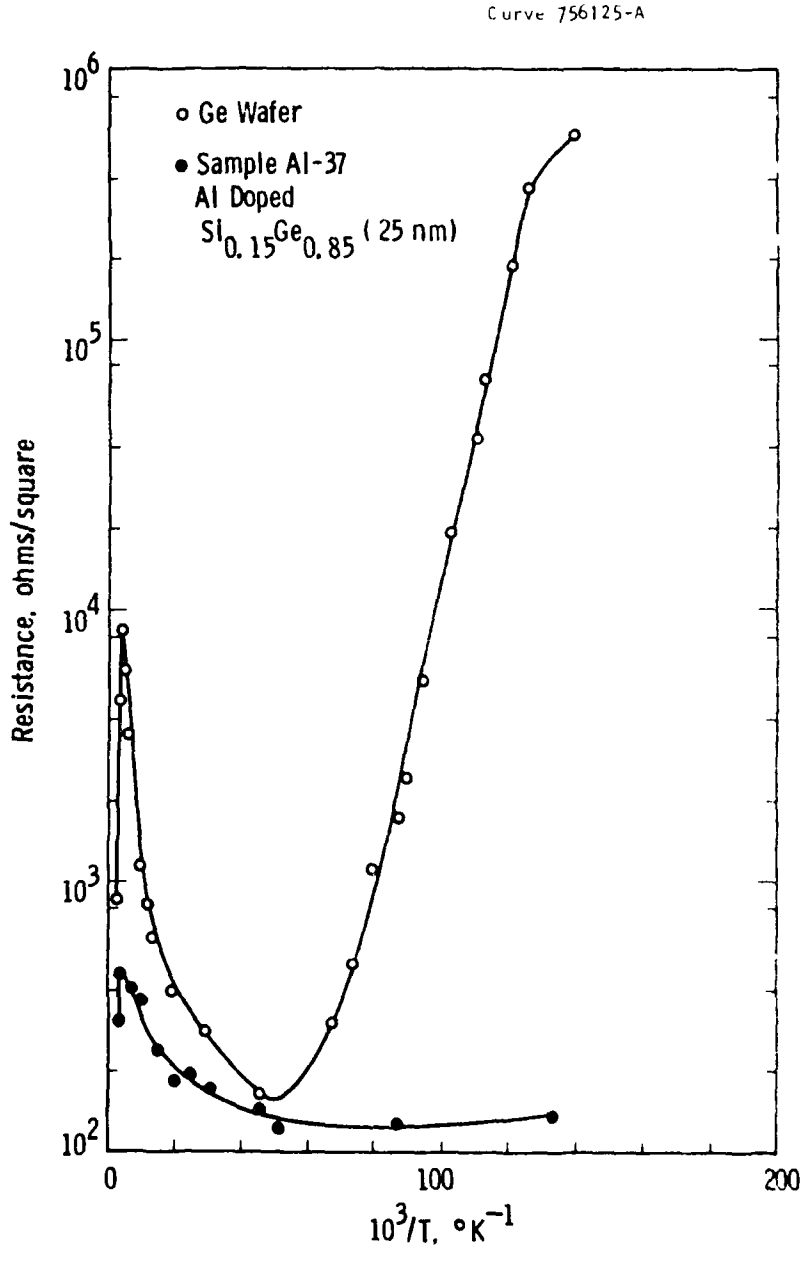

Figure 15. Resistance of substrate sample and of sample of Figure 14 versus temperature. Resistance obtained by Van der Pauw method is in ohms per square.

$N_s = 6 \times 10^{14}$ cm^{-2}. This implies a very heavy doping in the alloy layer. Even if the carriers were uniformly distributed throughout the 25 nm, the concentration would be 2.4×10^{20} cm^{-3}.

3.3.3 B-doped Structures

After learning of the calculations of the band offsets in Si_xGe_{1-x}/Ge heterostructures by R. People,[10] we recognized that it was not surprising that we observed no 2DHG in the Al-doped structures for which x = 0.15. A band offset of about 0.1 eV is required to trap a 2DHG in the Ge. People's calculation yields

$$\Delta E_v = [E_v(Ge) - E_v(Si_xGe_{1-x})] = 0.21x \text{ eV}.$$

Thus, for x = 0.15, the offset is predicted to be about 0.03 eV, which is too small to produce a 2DHG. For the B-doped samples we used x = 0.5. However, for this value of x, Bean's results[9] show that a maximum alloy thickness of 10 nm may be obtained for commensurate epitaxy. Since this thickness must include any undoped setback layer used to separate the 2DHG from the ionised acceptors, the mobility of the 2DHG may be limited to a value well below that observed in pure Ge.

A series of three structures were grown with a $Si_{0.5}Ge_{0.5}$ alloy layer 10 nm thick. Sample A had a uniformly doped alloy layer. Sample B had 2.5 nm setback layers on each side of a 5 nm doped layer. Sample C had a 2 nm uniformly doped layer sandwiched between two 4 nm thick undoped setback layers. Each sample had 100 nm of pure Ge epitaxially deposited on the wafer before the alloy was deposited, and a 200 nm thick cap layer of pure Ge.

The resistance in ohms per square is plotted for each of the samples in Figure 16 along with the corresponding data for the substrate. For each sample the resistance is much less than the wafer resistance for T < 10K. In the temperature range 12K < T <100K, the resistance of the three doped structures has approximately the same temperature dependence as that of the wafer. However, none of the doped samples shows a peak in the resistance near 250K as the wafer does. The

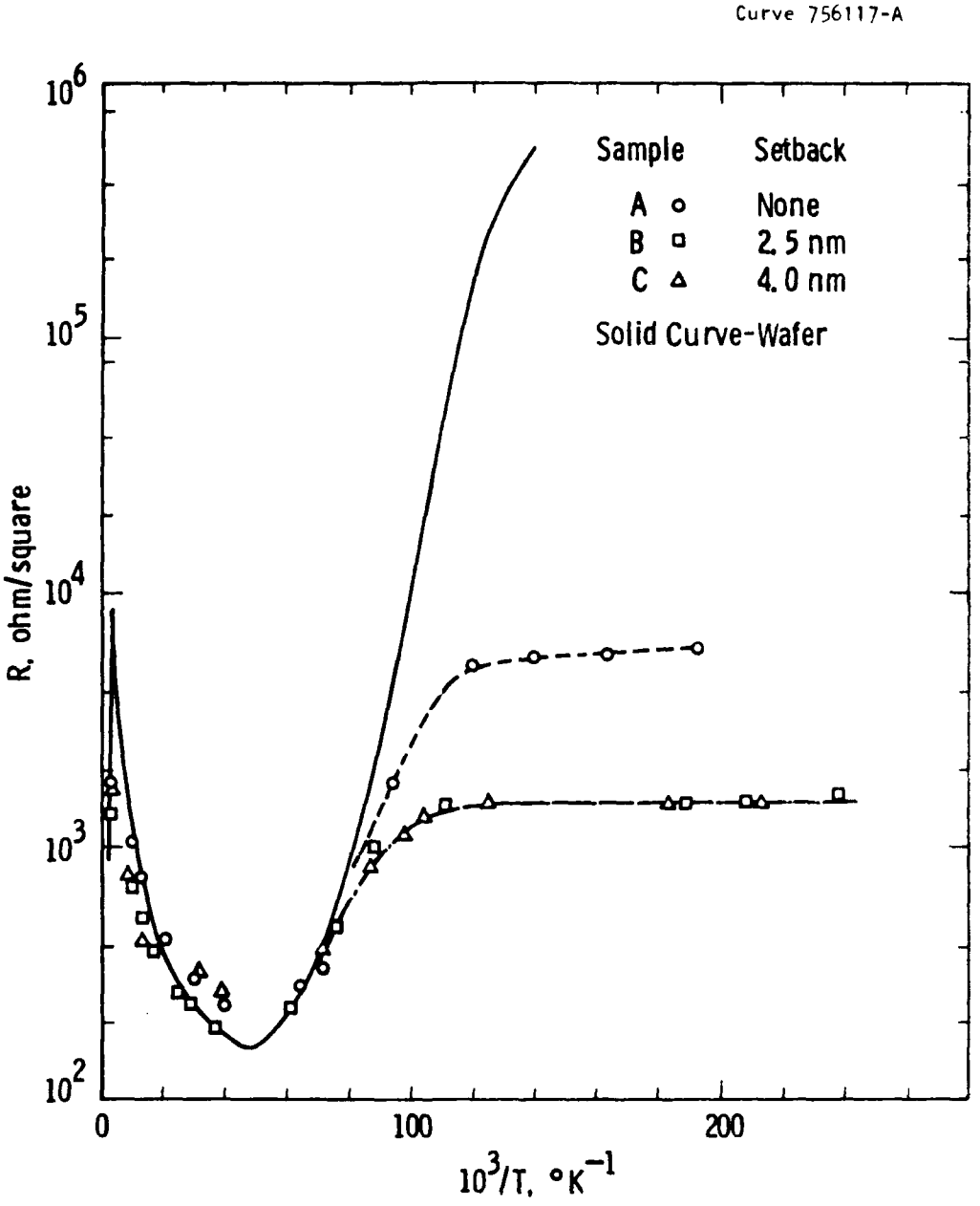

Figure 16. Resistance (ohms per square) for samples A, B, and C versus temperature. The resistance of the substrate is shown for comparison.

other feature of note is that the resistance of the three doped samples is constant below 8K, but that the sample with no setback has a resistance which is three times that of the two with setback. These data can all be explained in the following way. The resistance added in parallel with the wafer by the doped alloy, whether it be due to the carriers in the bulk alloy or a 2DHG, is roughly constant over the entire temperature range. At low temperatures this resistance is much less than the wafer resistance, and the alloy contribution dominates the conduction. At intermediate temperatures, the wafer resistance is lower and it dominates. Just below room temperature, where the wafer resistance peaks, the alloy conductivity dominates and no peak is observed.

If the resistance observed for $T < 8K$ in the three doped alloy samples was due to conductivity in the bulk of the alloy, we would expect a linear dependence on the alloy thickness. Thus, sample C should have ten times the resistance of sample A. The observed values can be interpreted as evidence for the existence of a 2DHG in the Ge. The higher resistance in sample A would be due to the increased scattering of the holes by the ionized acceptors which are nearby. As has been seen in GaAs/AlGaAs[11] and Ge_xSi_{1-x}/Si[4] structures, the setback layer separates the carriers from the ionized acceptors, decreases the scattering, and increases the mobility, which would decrease the resistance.

The Hall mobility calculated from the Hall voltage and the resistance measured by the Van der Pauw technique is plotted as a function of temperature for the doped samples and the wafer in Figure 17. As noted above, the mobility calculated in this way is not really meaningful where the substrate and alloy generate far different Hall voltages. However, for $T < 10K$ the measured values are due to the carriers provided by the doped layer because the wafer carriers are frozen out. The highest mobility is $\mu_H = 3.2 \times 10^3$ at $T = 4.2K$ in sample C. The mobility at $T = 4.2K$ decreases with spacer thickness as would be expected for a 2DHG. A minimum in the mobility for sample A occurs between 5 and 8K. It is not known whether the mobility of the

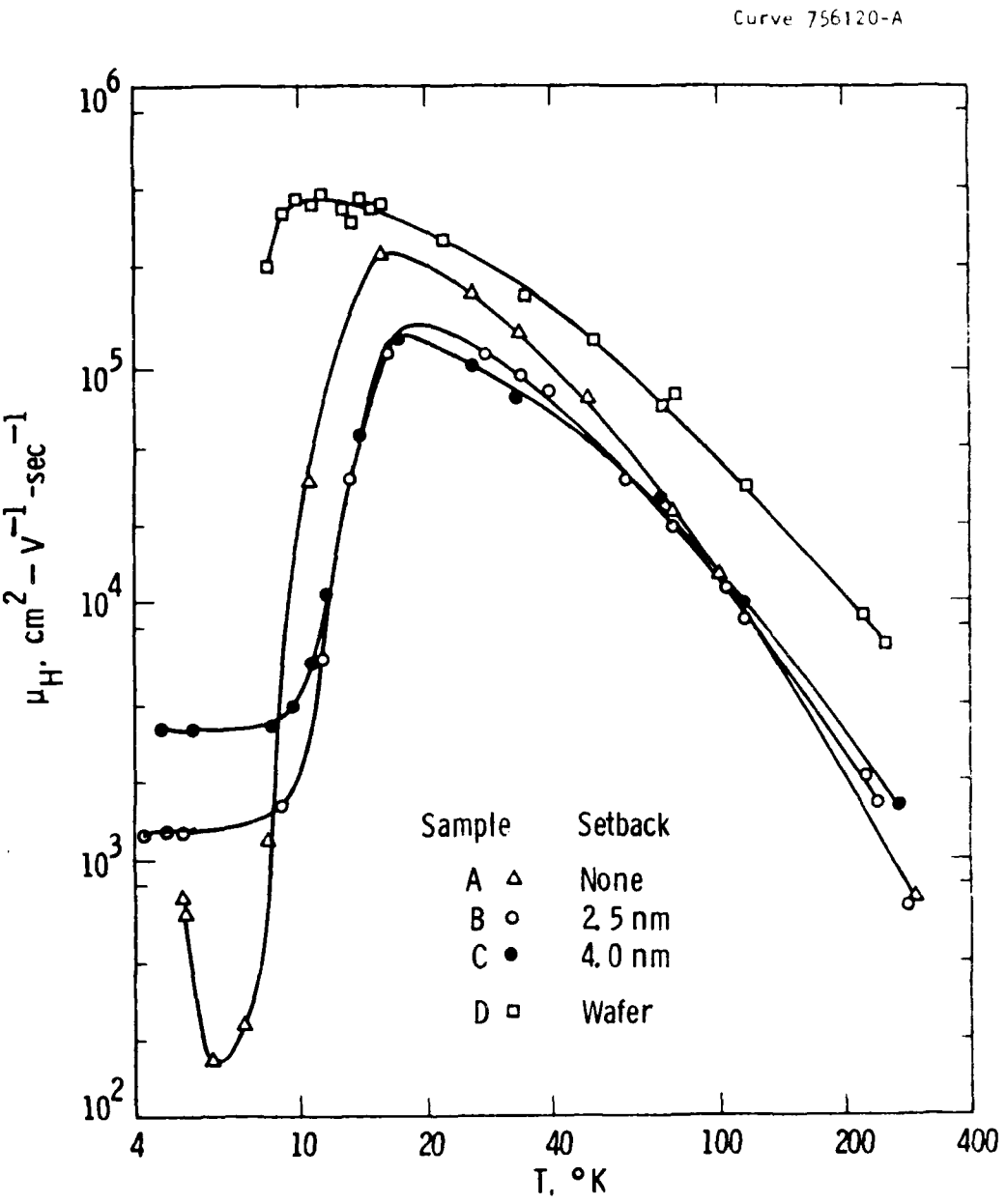

Figure 17. Hall mobility for samples A, B, and C versus temperature. R_H was obtained by Van der Pauw method with magnetic field normal to the (100) surface.

other two samples have a minimum in that temperature range because no data were taken. However, the increase for T below the minimum may be explained as due to the freeze-out of some carriers from the 2DHG onto the nearby ionized acceptors, making an effective spacer.

The sheet carrier densities obtained from the mobilities are $N_s(A) = 1.5 \times 10^{12}$ cm^{-2}, $N_s(B) = 3.2 \times 10^{12}$ cm^{-2}, and $N_s(C) = 1.3 \times 10^{12}$ cm^{-2}. The values for samples B and C scale with the thickness of the doped layer, as would be expected if the layer is completely depleted. However, the low value of N_s in sample A may indicate that the layer is not fully depleted. There are some holes frozen out on the acceptors with an effective barrier at the interface.

The important feature is that the observed dependence of mobility on spacer thickness is indicative of a 2DHG. The mobility values are not as large as would be expected for pure Ge, but are limited by scattering due to the proximity of the acceptors or ionized impurities of an unknown source. The value of 3.2×10^3 cm^2/V-sec for sample C at 4.2K is about the same as reported[4] in modulation-doped $Ge_{0.2}Si_{0.8}$/Si at 4.2K for a setback of 10 nm, and is greater than reported[5] for electrons in modulation-doped $Si_{0.5}Ge_{0.5}$/Si, where a 2.5 nm setback yields $\mu_H = 2.3$ cm^2/V-sec at 4.2K.

Shubnikov-de Haas oscillations were observed in samples B and C at T = 1.5K, but were not looked for in sample A. Figure 18 shows the magnetoresistance of sample C. The results for sample B were similar. The oscillations observed for B > 4 T are small in amplitude on top of the large background. Plotted in Figure 19 are the oscillations obtained by electronically subtracting a value given by $V = V_0 + V_1 B$ from the measured voltage. V_0 represents the B = 0 resistance value and V_1 represents the term which approximates the linear B dependence of the background magnetoresistence. After subtraction, the resulting voltage was amplified to yield the results given in Figure 19 for sample B. The oscillations are observed with the magnetic field normal to the plane of the alloy layer and the current. With the field applied in the plane the oscillations disappear. In addition, attempts were made to observe the oscillations in the longitudinal magnetoresistance and none were found.

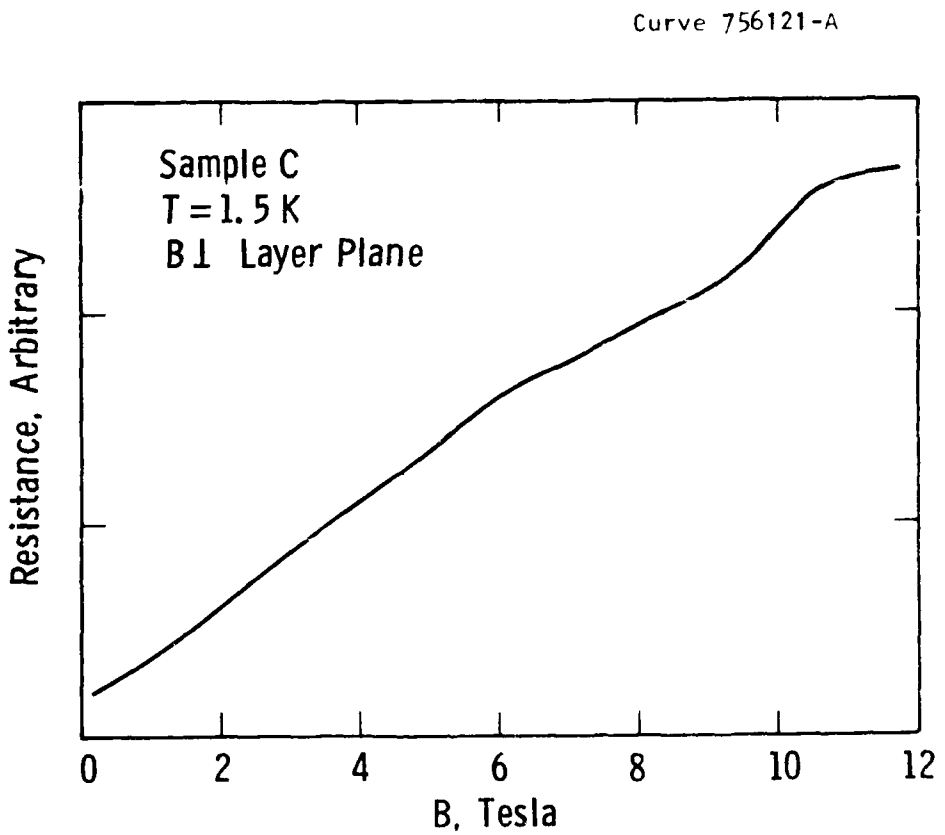

Figure 18. The transverse magnetoresistance of sample C (4.0 nm setback) versus magnetic field normal to the (100) surface.

Curve 756122-A

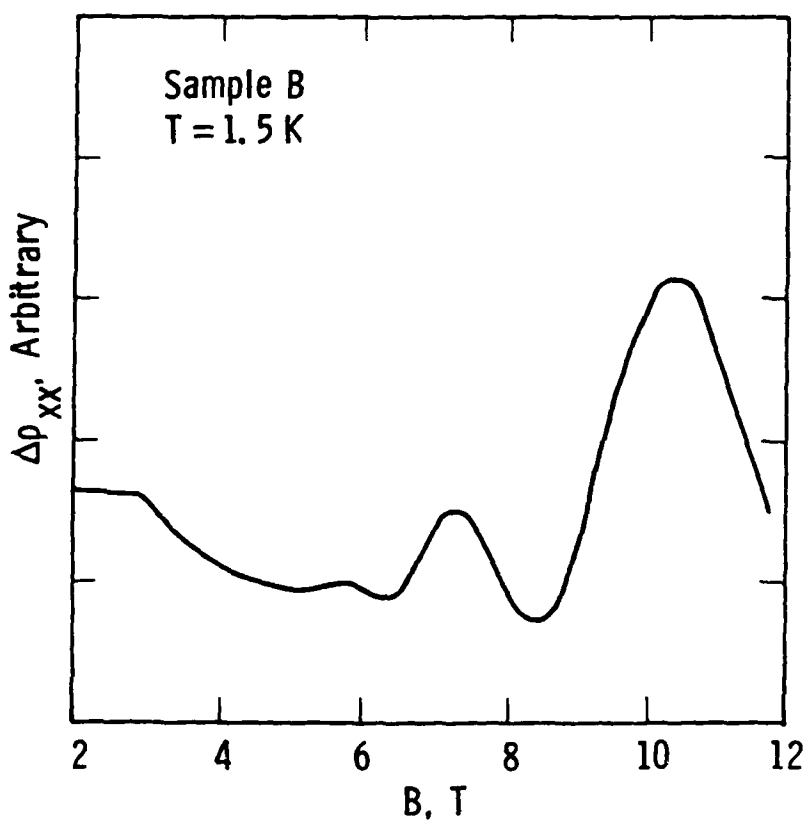

Figure 19. Oscillations in the transverse magnetoresistance obtained by electronically subtracting background of constant and linear term. Data are for sample B (2.5 nm setback) at T=1.5K with B normal to the (100) surface.

Magnetoresistance oscillations have been reported for both p- and n-type Ge.[12] However, in p-type the oscillations were observed only in the longitudinal magnetoresistence and not in the transverse case, whereas in n-type the reverse was true. Attempts to observe them in Si were unsuccessful.[12]

The high values of mobility observed in our samples at 4.2K, the dependence of the mobility on spacer thickness, and the obsevation of Shubnikov-de Haas oscillations in the transverse magnetoresistance all are evidence that the conduction is due to a 2DHG in the Ge.

The magnetoresistance data of Figure 19 are plotted versus 1/B in Figure 20. Shubnikov-de Haas oscillations should be periodic in 1/P and indeed the data show this. The period of the oscillations in Figure 20 is $\Delta(1/B) = 3.9 \times 10^{-2}\ T^{-1}$. The period depends only upon the carrier concentration. Modulation-doped structures of $Si/Si_{0.5}Ge_{0.5}$ in which the 2DEG is observed show a period of $2.8 \times 10^{-2}\ T^{-1}$ with a sheet charge density of $N_s = 3.0 \times 10^{12}\ cm^{-2}$. The period for our case yields $N_s = 2 \times 10^{12}\ cm^{-2}$, which is in reasonable agreement with the value of $3.2 \times 10^{12} cm^{-2}$ obtained from the resistance and Hall mobility data shown in Figures 16 and 17. It is possible to obtain the effective mass of the holes by observing the temperature and magnetic field dependences of the amplitude of the oscillations. We have not done this because of the inability to obtain lower temperatures in our cryostat.

3.3.4 Discussion and Conclusions

The variation of Hall mobility with spacer layer thickness and the observation of Shubnikov-de Haas oscillations with the magnetic field normal to the interface but not parallel to it are strong indications that the carriers form a 2DHG in the Ge at the interface in the B-doped $Si_{0.5}Ge_{0.5}/Ge$ heterostructures. The value of Hall mobility, $\mu_H = 3.2 \times 10^3\ cm^2/V\text{-sec}$, observed at T = 4.2K with a spacer layer thickness of 4.0 nm is not as high as might be expected in pure Ge, but is comparable to that observed for a 2DHG in the alloy in a Si_xGe_{1-x}/Si structure with a 10 nm undoped spacer. In that case the low-temperature mobility was thought to be limited by the presence of $\geq 10^{15}$ ionized

Curve 756126-A

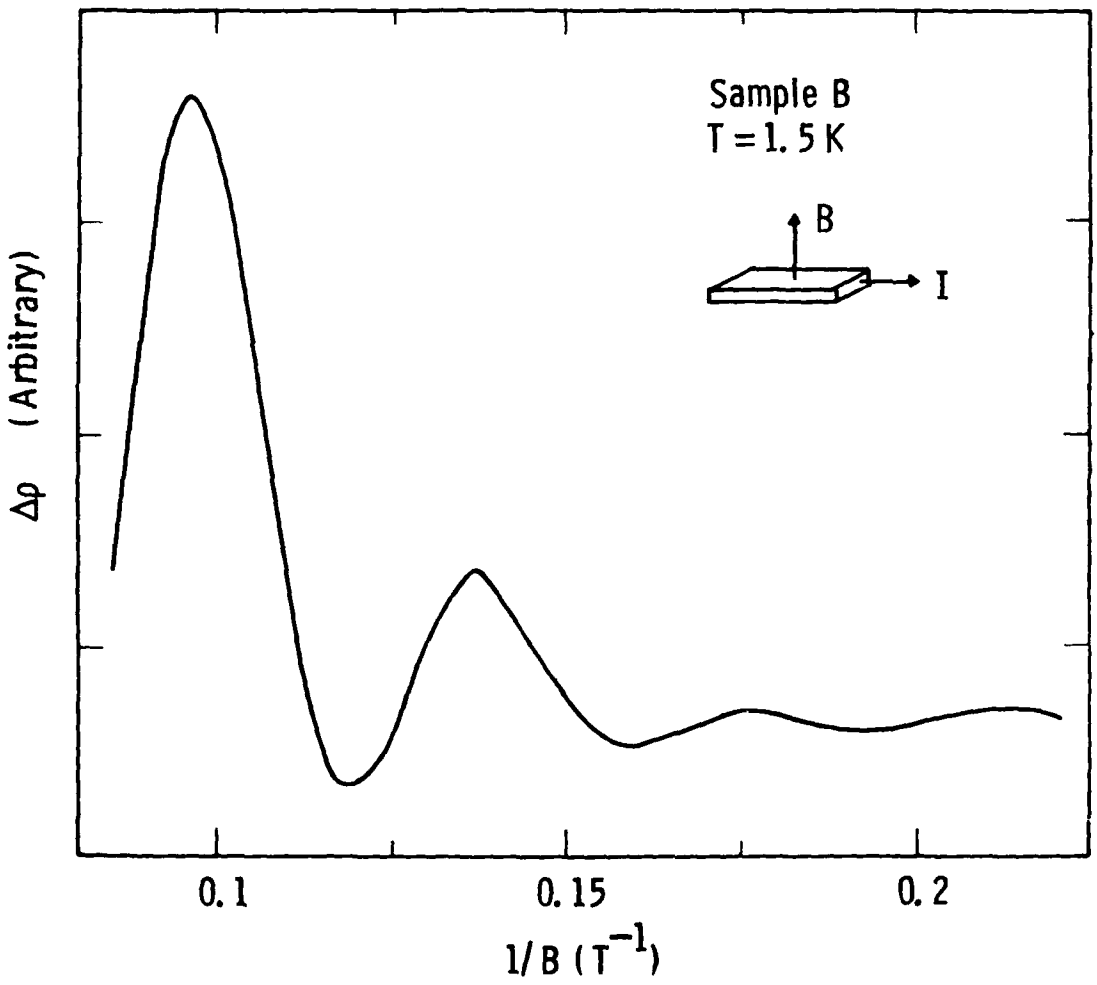

Figure 20. Transverse magnetoresistance of Figure 19 plotted versus reciprocal magnetic field.

impurities of unknown origin. Such may be the case for our samples as well.

The possibility that the observed mobility may be that of a highly degenerate hole gas in the bulk of the doped alloy layer can be ruled out. The hole mobility in both Ge and Si at these concentrations is far less than we have observed. In p-type Ge, μ_H varies[13] between 620 and 300 $cm^2/V\text{-sec}$ at 77K over the concentration range of 10^{18} to 10^{19} cm^{-3} and would not be higher at T = 4.2K. In p-type[14] Si at 4.2K, μ_H = 60 $cm^2/V\text{-sec}$ for a B doping of 10^{19} cm^{-3} and is much smaller for 10^{18} cm^{-3}.

We conclude that, based on the following observations, we have observed a 2DHG in the Ge:

a) The observed mobility is much greater than would be expected for a highly degenerate bulk conductor having 10^{18} to 10^{19} cm^{-3} carriers.

b) The observed increase in mobility with spacer layer thickness would not occur for bulk conduction.

c) The observed dependence of the sample resistance on spacer layer thickness cannot be explained by the bulk conduction.

d) Our results are very similar to those in $Ge_{0.2}Si_{0.8}/Si$.

e) Oscillations are observed only in the longitudinal magnetoresistance of bulk Ge and not at all in bulk Si.

f) The observed Shubnikov de Haas oscillations indicate a 2DHG and the oscillation period is consistent with the sheet carrier density obtained from the Hall data and the known doping level.

4. ACKNOWLEDGMENTS

The authors are pleased to thank Dr. G. T. Mallick, Jr. for the design of the electronic circuit used for extracting the Shubnikov de Haas oscillations from the magnetoresistance; Dr. D. L. Meier and Dr. M. H. Hanes for the spreading resistance measurements; Dr. J. Talvacchio and R. D. Blaugher for many helpful discussions; and J. H. Uphoff and J. Buttyan for valuable experimental help.

5. REFERENCES

1. For a review see Low Temperature Electronics, ed. by R. K. Kirschman, IEEE Press, N.Y., 1986.

2. M. Heiblum et al., Phys. Rev. Lett. 55, 2200 (1985); A.F.J. Levi et al., Ibid. 55, 2071 (1985).

3. D. M. Brown and R. Bray, Phys. Rev. 127, 1593 (1962); P. P. Debye and E. M. Conwell, Phys. Rev. 93, 693 (1954).

4. T. P. Pearsall et al., Proc. 1st Int. Symp. on Si MBE, J. C. Bean, Ed., Electrochemical Soc., Pennington, N. J., p. 400 (1985).

5. H. Daembkes et al., IEEE Trans. on Elect. Dev. ED-33 (1986).

6. J. Talvacchio et al., Proc. of ICMC, Adv. in Cryo. Res. 32, 527 (1986).

7. D. E. Aspnes and A. A. Studna, Appl. Phys. Lett. 39, 316 (1981).

8. R. M. Ostrom and F. G. Allen, Appl. Phys. Lett. 48, 221 (1986).

9. J. C. Bean, in Ref. 4, p. 337.

10. R. People, Phys. Rev. B34, (1986).

11. See, for example, M. Heiblum et al., Appl. Phys. Lett. 44, 1064 (1984).

12. W. Bernard et al., Phys. Rev. 135, A1386 (1964).

13. O. A. Golikova et al., Sov. Phys. Sol. State 3, 2259 (1962).

14. F. J. Morin and J. P. Maita, Phys. Rev. 98, 28 (1954).